ASSESSMENT OF ANTIOXIDANT AND ANTIBACTERIAL ACTIVITIES OF IRON-TITANIUM OXIDE NANOPARTICLES SYNTHESIZED IN VARIOUS SOLVENTS AND THEIR MICROSCOPIC CHARACTERIZATION

M. Arshad, A. Qayyum[*]and S.J. Muhammad[**]

Department of Chemistry, Govt. Post Graduate Islamia College, Gujaranawala
[*]Department of Chemistry, University of Agriculture, Faisalabad
[**]Institute of Chemistry, University of the Punjab, Lahore-Pakistan
[*]Corresponding author’s E-mail: sarafatima1093@gmail.com

ABSTRACT: Iron doped Titanium oxide (Fe/TiO_2) nanoparticles with size about 9-16 nm was synthesized by sol-gel assay based on various solvents followed by calcination for 3 hours at 700^{o}C. The properties of the doped materials were compared in various solvents in sense of antibacterial and antioxidant behavior. Antibacterial and antioxidant potential of all synthesized nanoparticles were studiedviadisc diffusion method and free radical scavenging potential of stable 1,1- Diphenyl-2-picryl hydrazyl respectively. Result of antibacterial activity was found in the range of 7.5-10 mg/disc which shows that effect of various solvents play an important role on the antibacterial activities of Fe-doped TiO_2 nanoparticles. The characterization of all synthesized nanoparticles was performed by various characterization techniques such as Thermo gravimeteric analysis (TGA), Fourier transform infra-red (FT-IR), Scanning electron microscope (SEM), Dynamic light scattering (DLS), X-ray diffraction (XRD), Photoluminescence (PL) analysis and UV-Vis spectrometer. The Fe/TiO_2 nanoparticles also showed significant antioxidant activity (20-27%).

Key words: Antibacterial, Antioxidant, Nanoparticle, Synthesis and Characterization.

(Received 01-04-2018 Accepted 05-06-2018)

INTRODUCTION

The role of antioxidants in the scavenging of free radicals is of great importance. The major useful functionsof antioxidant are to inhibit the oxidative reactions in various fields such aspharmaceutical, cosmetic, food and the disease associated with stress. Microbial activities are also significant issue in the pharmaceutical, cosmetic and food industries (Hajipour *et al*., 2012, Rehman *et al*., 2017). The increase in the use of organic natural food stuff and increasing origins of increase bacterial response to prevailingstabilizersthan other sources have been encouraged by food researchersto find natural antibacterial substances. Titania (TiO_2) is the most important material which is being used for different applications due to its optical potential, stability, comparatively less production cost and high refractive index (Stan *et al*., 2015). Due to its surface photochemistry along with chemical and physical stability of semiconductor, it has multiple applications especially for self-cleaning (Carnio *et al*., 2007), water treatment (Lachheb *et al*., 2002), air purification (Yu *et al*., 2007), anti-bacterial (Zhang *et al*., 2006), sensors (Rella *et al*., 2007), solar energy conversion (Jung *et al*., 2005) and anti-ultraviolet agent (Hoffmann *et al*., 1996). Photocatalytic characteristics of TiO_2 based on the available composition, area of surface, crystallinity degree and actives sides (Fujishima and Honda 1972; Asahi *et al*., 2001; Yu *et al*., 2002; Li *et al*., 2004; Zhu *et al*., 2004; Thompson *et al*., 2006; Chen *et al*., 2007; Fujishima*et al*., 2008; Yang *et al*., 2008; Zhang *et al*., 2008). Sontake*et al*. (2012) reported photo catalytic inactivation of gram negative bacteria by TiO_2 nanoparticles in the incidence of visible light. Brookite, anatase and rutile are three basic crystalline structures of TiO_2 (Testino *et al*., 2007). Brookite and anatase are metastable while rutile is most stable phase. Now-a-days synthesis of nanoparticles of rutile is getting more attention because of its excellent photo catalytic behavior (Dessombz *et al*., 2007; Testino *et al*., 2007; Wang *et al*., 2007; Wang *et al*., 2009; Arshad *et al*., 2018). TiO_2 with band gap energy 3.2 e.v need UV light source to be photo activated. Researchers are trying to improve the band gap of TiO_2 which is most advanced synthesis method that include the doping of TiO_2 with other transitions elements like V (Tsuyumoto *et al*., 2008), Fe (Tojo *et al*., 2008, Naeem *et al*., 2010 Mangham 2011), MO (Du *et al*., 2006), Co (Subramanian *et al*., 2008; Sarkar *et al*., 2011), AU (Zhou *et al*., 2011) and with nonmetals such as N (Fu *et al*., 2012), P (Lv *et al*., 2009), S (Umebayashi *et al*., 2002), F (Dozzi*et al*., 2017).Among all these radius of iron Fe^{3+} (0.64A^o) is similar to Ti(0.68A^o) and it therefore easily doped with TiO_2enstal (Zhou *et al*., 2006).

The dopant (Fe^{3+}) behaves as charge trapper that enhance photo catalysis rate in a suitable range (Zhang *et* *al*., 2010). Fe^{3+} is considered best dopant that is most widely used for TiO_2 (Weng *et al*., 2005; Hou *et al*., 2009; Wang *et al*., 2009; Zhang *et al*., 2009; Yalc *et al*., 2010; Jia *et al*., 2011; Naceur *et al*., 2011; Su *et al*., 2011). Zhang *et al*. (2009) synthesized Fe doped TiO_2 nanoparticles which are commend doped Fe converted into Fe^{3+}that have active trapper of e^- or h^+. Due to this reason it decreases the rate of recombination of e^-/h^+.

The combination of Fe^{3+} ions with -OH group on TiO_2 nanoparticles surface lead to the formation of Fe^{3+}(OH) complex that is good electron transfer source (Wang *et al*., 2008).Various methods are being used for the synthesis of Fe-doped TiO_2 nanoparticles. Sol gel (Attar *et al*., 2006), ball milling (Babaei *et al*., 2006), chemical vapor deposition (Ahmadi *et al*., 2006) and micro emulsion (Haghighat *et al*., 2006) are well known methods.

In current study, the synthesis of Fe-doped TiO_2 nanoparticles was done at low temperature through deposition sol-gel method by using titanium isopropoxide (TTIP) in aqueous acidic media. The purpose of current work was to study the effect of solvent on surface area, photoluminescence study. Biological activities like antibacterial and antioxidant of synthesized nanoparticles were also investigated.

MATERIALS AND METHODS

This study was designed to synthesize the nanoparticles Fe-doped Titinium Oxide and their characterization such as FT-IR, XRD, SEM, TGA, PLA and DLS. The biological activities like antibacterial and antioxidant of synthesized Fe-doped Titinium Oxide nanoparticles were further investigated based on different solvents such as acetonitrile, n-Hexane and isopropyl alcohol.

Analytical instruments: Various instruments were used for the characterization of synthesized Fe/TiO_2 nanoparticles are UV/Vis Spectrophotometer UV-1700 (Shimadzu), FESEM (JEOL 7600), FTIR (shimadzu), XRD (Philips X' Pert), TGA/SDT (G600 V8.3 Build), Oven (EV 108 Ac-Kapa) and PL-Spectra (Hitachi F-7000).

Reagents and chemicals: Analytical grade chemicals such as tartaric acid, (Panreac), $FeCl_3.6H_2O$(Merck), 2propanol(Fisher), acetonitrile(Merck), n-Hexane(Fisher), HNO_3 (Fluka) and Titanium isopropoxide (Aldrich) were used in this study without any further purification. Double distilled water was used throughout this study.

Synthesis procedure

Synthesis of Fe doped TiO_2 nanoparticles: Fe doped TiO_2 nanoparticles were synthesized viasol-gel assay. First of all 20 ml of isopropyl alcohol and 10 ml of titanium isopropoxide (TTIP) were mixed as precursor for the synthesis of TiO_2. The solution was stirred for twenty minutes at room temperature. This process was exothermic (pH = 2). Now added (0.540g) of $FeCl_3.6H_2O$ (0.1M) in 20 ml of isopropyl alcohol and added this solution in the above prepared solution by mixing both solution (pH = 3). Now added concentrated HNO_3 drop wise to form the acidic media as hydrolysis catalyst, the mixture was transparent at this condition. Now added NH_3(4M):H_2O drop wise into the solution until the pH reached about 6.2. The solution was stirred for 4 hours on hot plate with condenser at temperature 75°C followed by centrifugation for 30 minutes at 250 rpm. The separation of precipitates followed by several times washing with double distilled water and drying at 80°C for 3 hours and then calcined at 700°C for 3 hours. Same procedure is repeated for the synthesis of Fe/TiO_2 nanoparticles by using different solvents with same molar concentration (Arshad *et al*., 2016).

Antibacterial activity of Fe doped TiO_2 nanoparticles: Both gram positive and gram negative bacteria *Escherichia coli* and *Staphylococcus aureous* respectively used for the examination of antibacterial activity of synthesized nanoparticles. This activity was performed by assay used by Afzal *et al*. (2014) and Qayyum *et al*. (2016) with slight modification. Firstly parti dishes was autoclaved and then washed by doubled distilled water. Again petridished was autoclaved at 121˚C.13 g/L of nutrient medium in pure cultures form was maintained in petri dishes followed by suspension in double distilled water and homogenously distribution. The inoculation (100 µL/100 mL) was mixed with medium and transferred in these sterilized petri plates. The bacterial strains were diverse in above nutrients in separate labeled petri dishes agar medium followed by sterilization by autoclaving at 121˚C for 15 min. Then allowed this mixture at room temperature, gel like stuff was formed. Some well was developed according to all required examined samples. 100µL of different form (M_3, M_4, M_5) of synthesized nanoparticles and standard was added in these different well which were properly labeled. The petri plates were then incubated at 37˚C for 24 hours, for the growth of bacteria. After that, inhibition zones were measured by zone reader and recorded in millimeters.

Determination of antioxidant activity by DDPH free radical scavenging assay: Antioxidant activity of synthesized nanoparticles was determined by scavenging the free radical of 1,1- Diphenyl-2-picryl hydrazyl (DPPH) by using the method used by Chikhi *et al,* (2012) and Jain *et al,* (2011). N-hexane solvent was used for the preparation of samples and ascorbic acid was used as standard in this study. 2 mL of each sample and standard was separately mixed with solution of DPPH (0.002%).

These solutions were incubated for 30 minutes. After incubation the absorbance was measured at 517 nm wavelength. N-hexane was used as blank. Antioxidant activity of each sample was calculated according to following formula

$$I\,\% = (A_{blank} - A_{sample}/A_{blank}) \times 100$$

In this formula, absorbance of blank was shown by A_{blank}while absorbance of each tested sample was shown by A_{sample}.

RESULTS AND DISCUSSION

The presence study was focused on the synthesis of Fe doped Titnium nanoparticles. The different characterization such as FT-IR, XRD, SEM, TEM, DLS, Photoluminescence analysis were also investigated while the biological activities including antibacterial and antioxidant activities.

Characterization of Fe doped TiO_2 nanoparticles: FTIR Characterization: The FT-IR spectra of TiO_2 nanoparticles were analyzed and given in figure (1). Many absorption bands appear in the spectra that belongto the organic groups such as hydroxyl and alkane. The broad band appear at ~ 3400 cm^{-1} to 3500 cm^{-1} belongs indicate the stretching vibration of the hydroxyl group (OH^-) representing the water as moisture. The peak at ~ 1631 cm^{-1} indicates the bending vibration of absorbed water. The bonds at ~ 2900-3000 cm^{-1} appear because of organic residues that originate by the sample preparation method. The peak which appears in the 800 cm^{-1} to 450 cm^{-1} range belongs to Ti – O – Stretching bands. After calcinations of TiO_2 sample, almost all peaks of hydroxyl and titanium carboxilate disappeared, only peaks between 800 and 450 cm^{-1} remained, which shows the formation of TiO_2 nanoparticles.

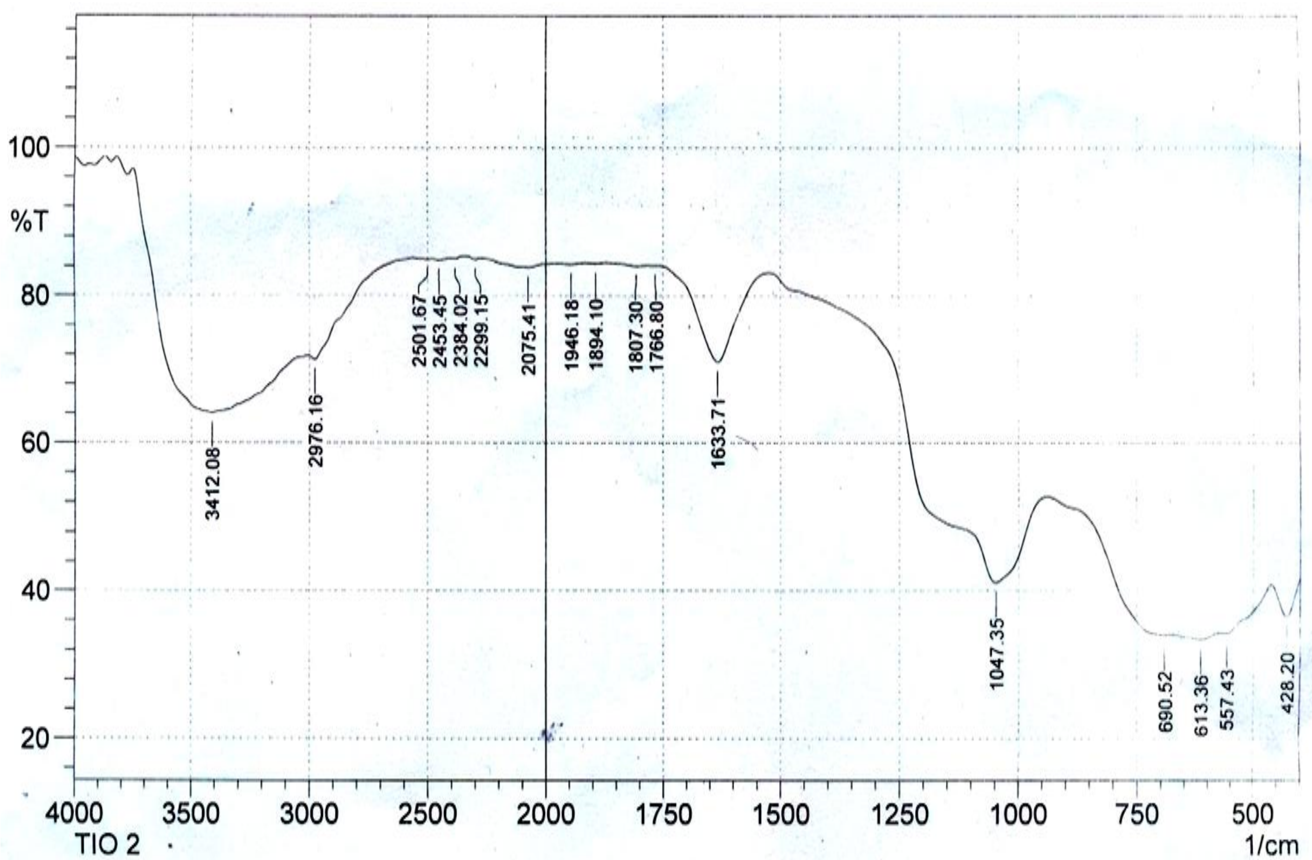

Figure-1: FTIR Spectra of pure TiO_2

Figure-2 showed that FT-IR spectra of doping of 0.1M concentration of Fe of TiO_2 doped with. Spectra showed that as intensity of the peak increases, the broad bands at 2350 – 3500 cm^{-1} which indicate O – H for absorbed water molecules lead to the formation of Ti-OH. It showed that as the concentration of Fe increased in the solution, the hydroxyl contents also increased, accordingly.

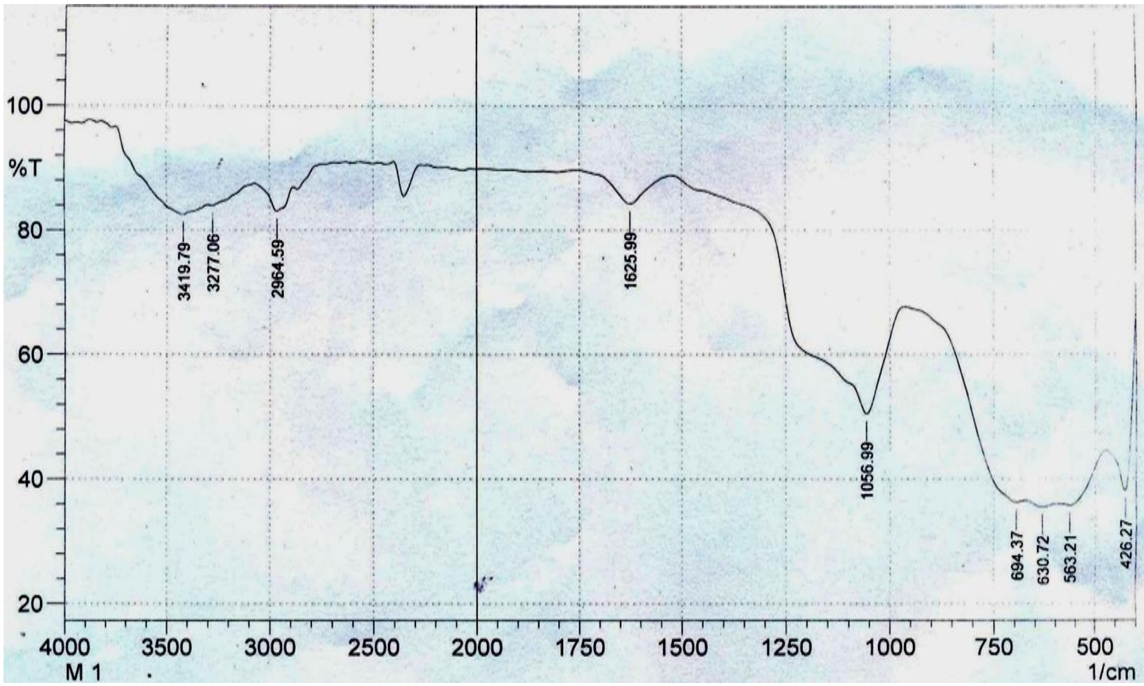

Figure-2: FTIR Spectra of 0.1M Fe-doped TiO_2 nanoparticles

XRD analysis: The crystallite size and phase composition of synthesized nanoparticles were studied by X-ray diffraction analysis. Figure (3) showed the XRD patterns for pure TiO_2. Results shows that particles were mostly comprised of rutile structure with tetragonal shape. Essentials peaks of pure TiO_2 nanoparticles were found at 2θ = 27.46°, 36.05°, 41.22°, 44.05°, 54.33°, 56.63°, 62.72°, 64.03° and 69.76° with planes of (110), (101), (111), (210), (211), (220), (002), (310) and (112) respectively. Which are all well indexed with PDS # 00-004-0551. Tetragonal rutile structure of TiO_2 was shown by these results. Average particle size of TiO_2 was calculated by using the Scherrer's equation as explained by Eq. 1

$$D = \frac{k\lambda}{\beta(\cos\theta)} \quad \text{(Eq.1)}$$

In the above equation,
D = average crystallite size
β= broadening of peak
k = grain shape dependentconstant (k = 0.89)
θ = diffraction angle.
λ = wavelength (nm) of incident radiations

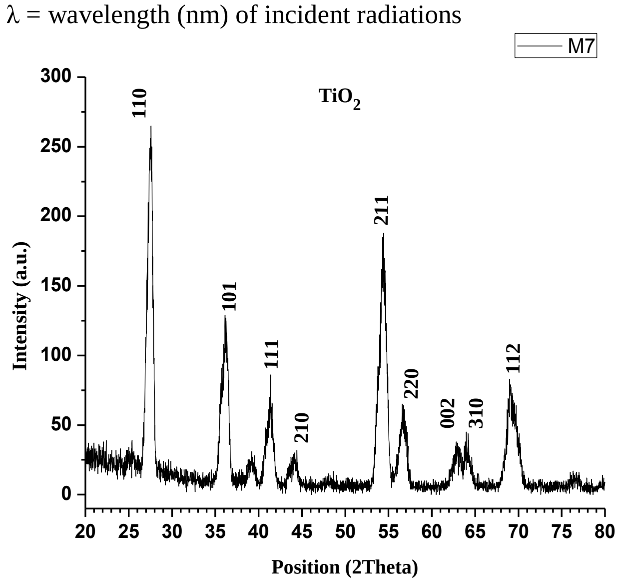

Figure-3: XRD Spectra of Pure TiO_2 nanoparticles

Figure-4 show the XRD pattern of 0.1M Fe-doped TiO_2 nanoparticles synthesized in 2-propanol by sol-gel method the analysis was carried out in 2θ range of 20° – 80°. Figure-3 showed that all synthesized nanoparticles in various solvent were found of rutile behavior of TiO_2 diffraction peaks (PDF # 00-004-0551) containing no impurity phase. After doping of Fe, peak position of (101) shift to a larger angle. This shows that position of Ti ions in TiO_2 was just replaced by doped Fe without possessing any change in crystal. Fe-doped TiO_2 nanoparticles synthesized in 2-propanol show the characteristics peaks at 2θ = 32.5°, 33.2°, 35.96°, 41.01°, 43.67°, 49.26°, 54.35°, 56.61°, 62.78°, 63.96° and 69.37° with diffraction planes (101), (104), (110), (021), (202), (024), (116), (018), (027), (300) and (208) respectively.

XRD analysis determined the full width, position and intensity of peaks by using the Scherrer formula as explained in figure (4). Average size of nanoparticles was calculated about 9.42nm in 2-propanol, 6.36nm in acetonitrile and 16.05nm in n-Hexane which are close to the DLS Analysis.

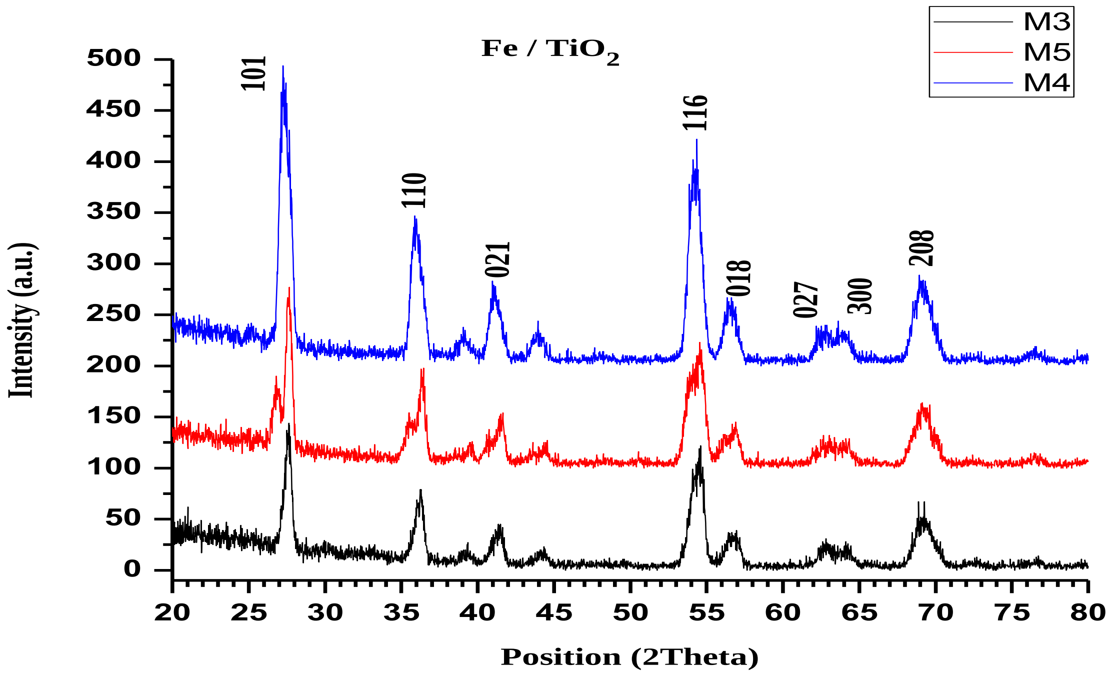

Figure-4: XRD patterns of Fe-doped TiO_2

SEM Analysis: Figure-5a show the SEM analysis of nanoparticles synthesized by 0.1M Fe-doped TiO_2 by sol-gel method using different solvents. Figure (5a) show that all particles are inter-connected, spherical that form open, porous, network. Figure (5b, 5c) showed heterogeneous, porous surface morphology of Fe-doped TiO_2 nanoparticles synthesized in acetonitrile and n-hexane.

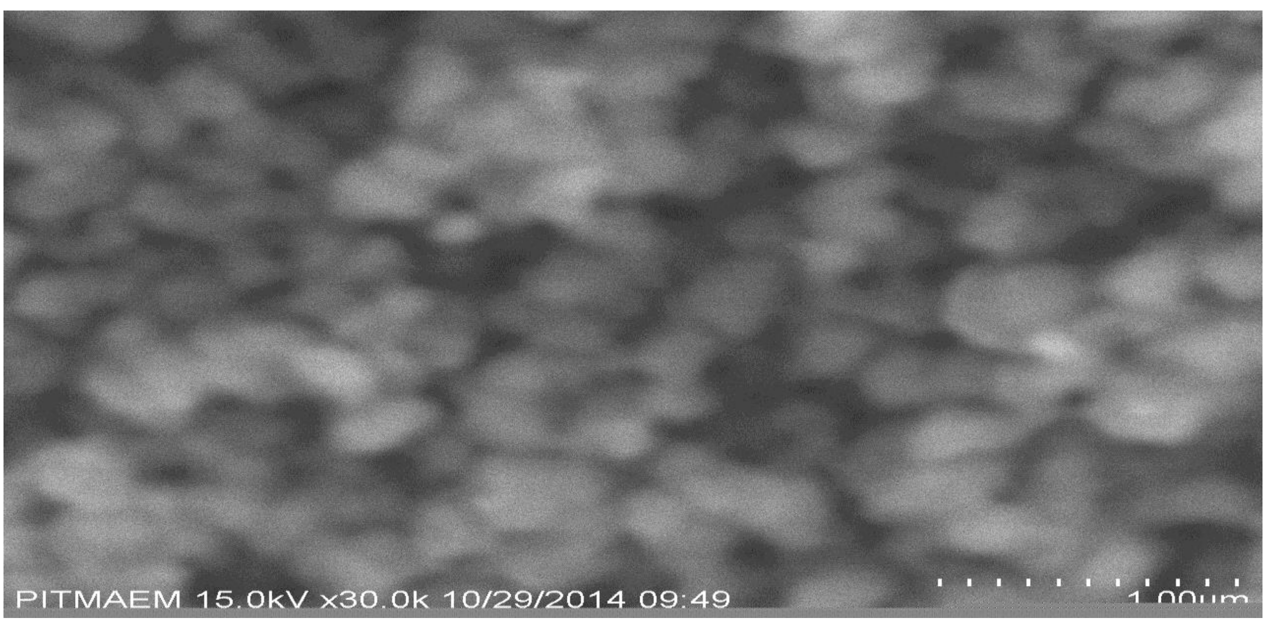

Figure-5a: SEM image of Fe-TiO_2 nanoparticles (2-propanol)

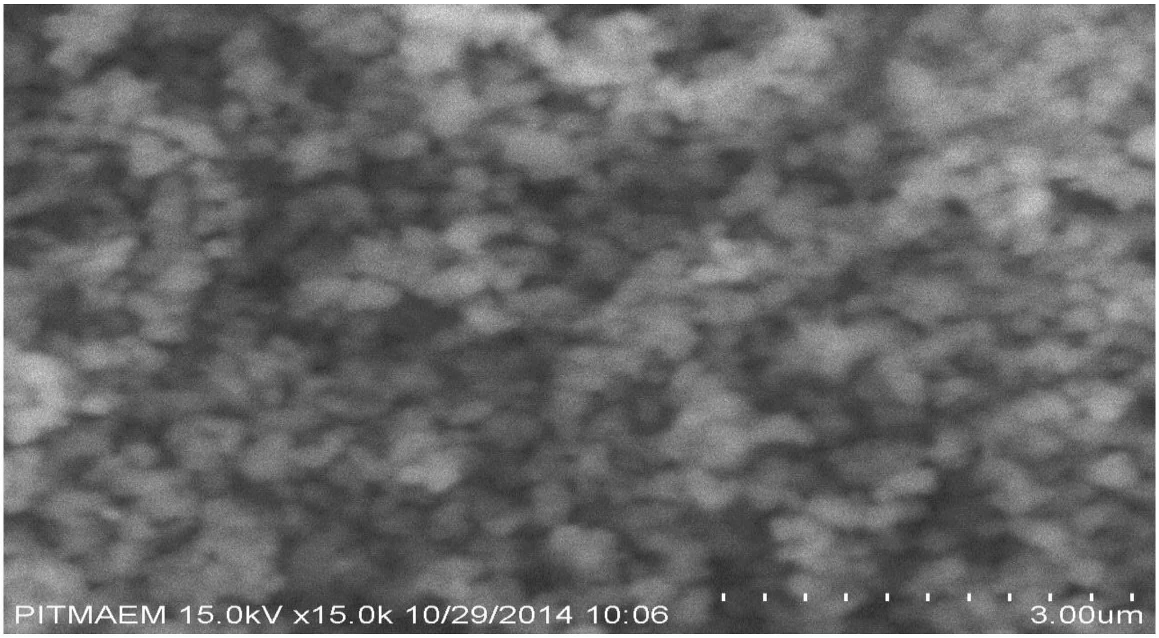

Figure-5b: SEM image of Fe-TiO_2 nanoparticles (Acetonitrile)

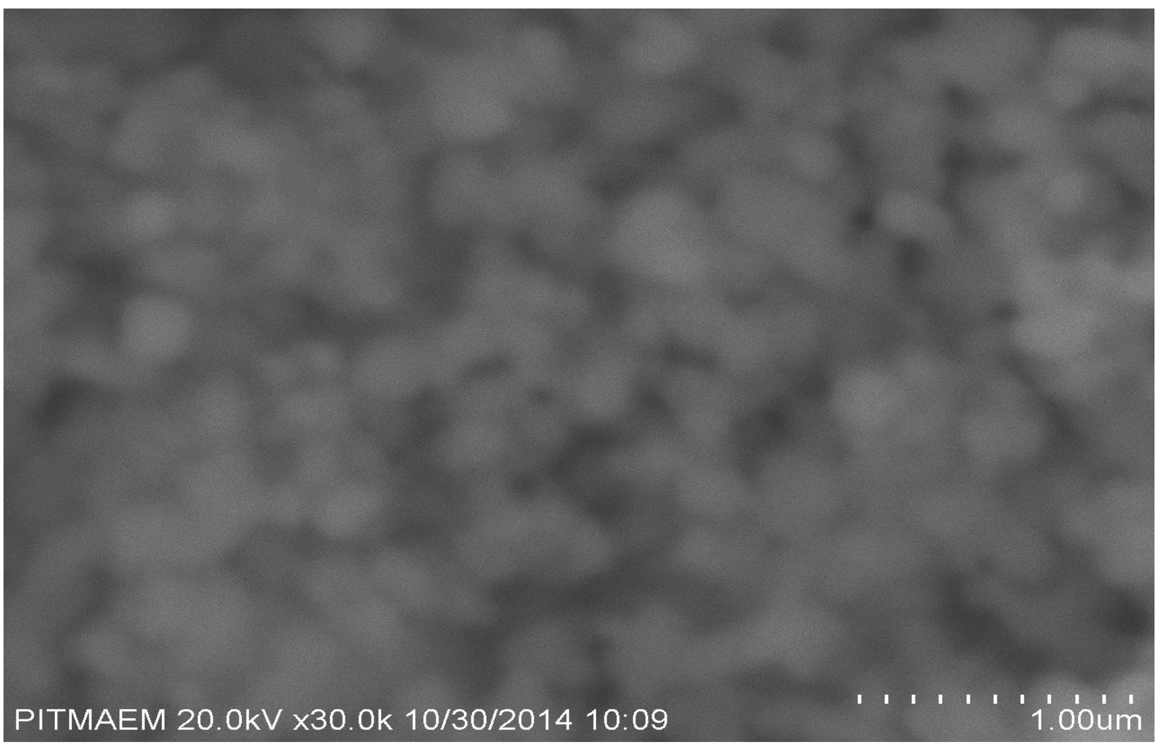

Figure-5c: SEM image of Fe-TiO_2 nanoparticles (n-Hexane)

TGA analysis: Figure-6 show the TGA-DSC curves of Fe-doped TiO_2 nanoparticles calcinated at 700°C. It shows the mass losses in steps and thermal events corresponding to these losses which may be due to any physical phenomena. The TGA show that the mass loss is about 12% up to 490°C. This loss is due to presence of H_2O, OH are may be due to the iron as doping in the TiO_2 nanoparticles which lowered thedegrading temperature. An endothermic peaks at 75°C in figure 6may arise due to the loss of water whereas the exothermic peak appeared at 230°C is recognized to thermal decomposition of organic matter and sintering between the TiO_2 nanoparticles.

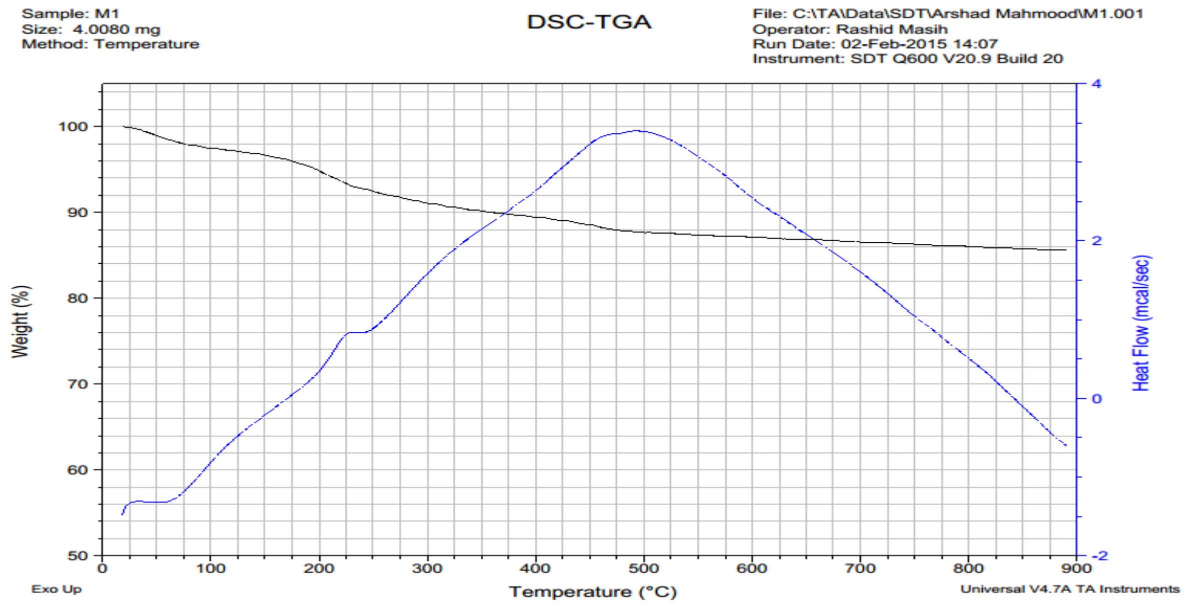

Figure-6: TGA Spectra of Fe-doped TiO_2

DLS Analysis: Figure-7 showed the DLS analysis of Fe-doped TiO_2 nanoparticles which determined the hydrodynamic diameter nanoparticle, which was found larger than their size. It may be because of occurrence of stabilizer at surface of dopant.

Table-1: Effect of various solvents on the size of Fe/ TiO_2 nanoparticles.

Solvent No.	Method	Temperature	Calcination Time	Stirring Time	Solvent	Zeta-size	Peak-I
M_3	Sol-gel method	80°C	700°	3 hours	2-propanol	9.27	824.91
M_4		80°C	700°	3 hours	Acetonitrile	8.45	824.91
M_5		80°C	700°	3 hours	n-Hexane	10.94	458.66

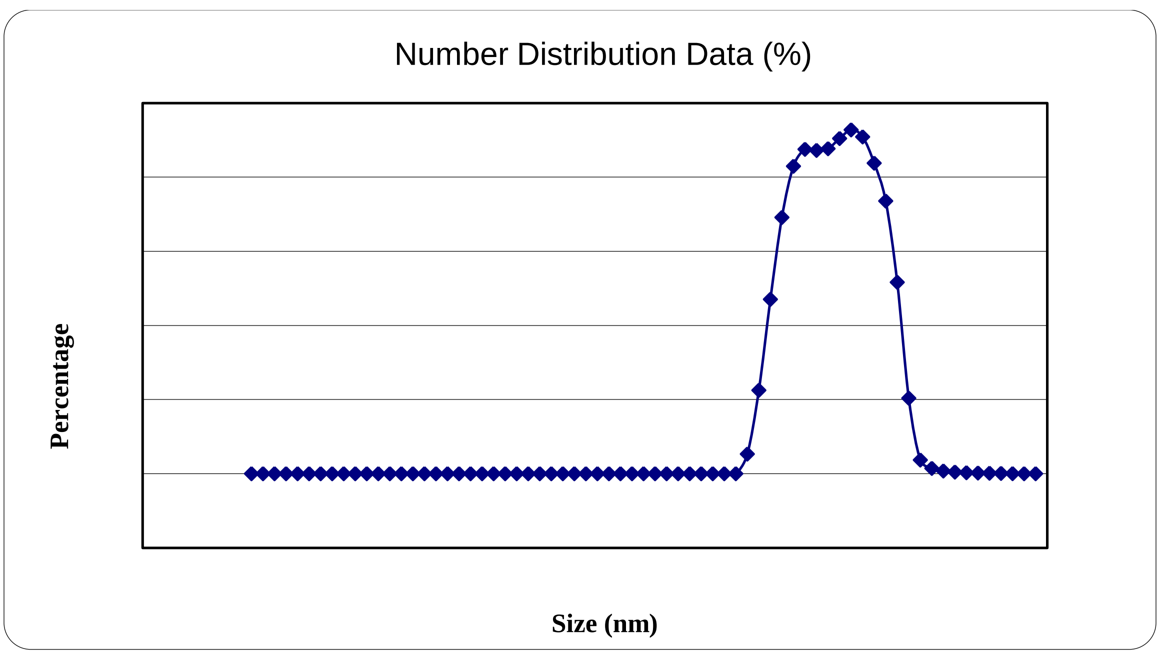

Figure-7: DLS Spectra of 0.1M Fe-doped TiO_2 Nanoparticles, (2-Propanol)

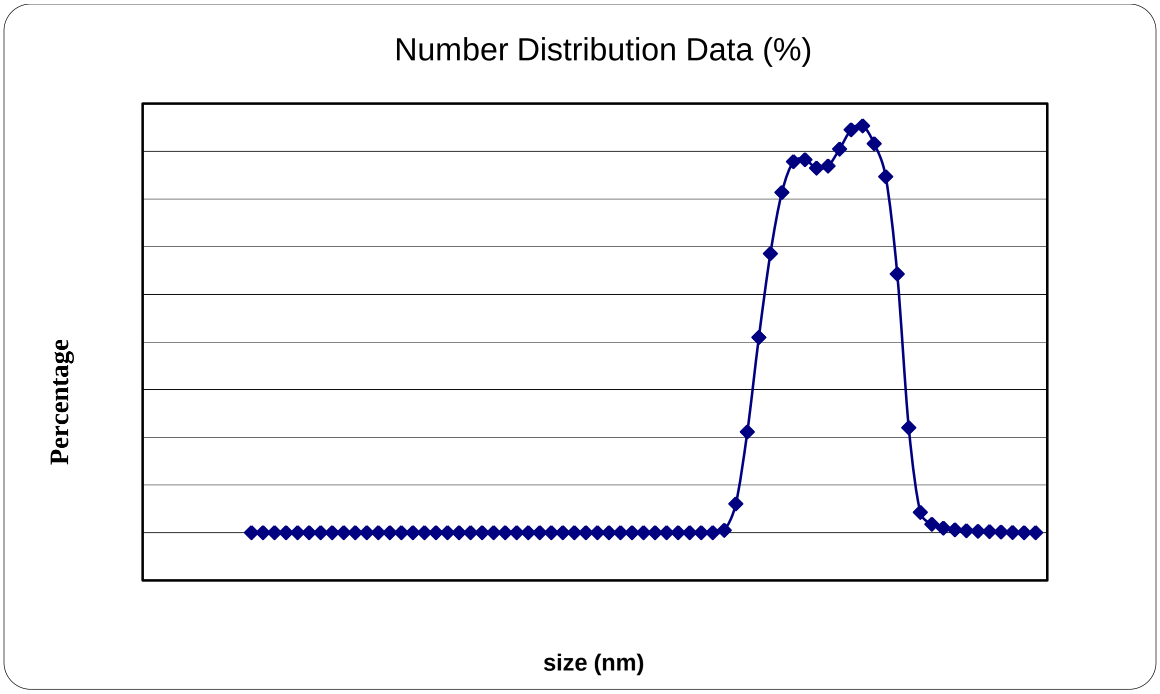

Figure-8: DLS Spectra of 0.1M Fe-doped TiO_2 Nanoparticles, (Acetonitrile)

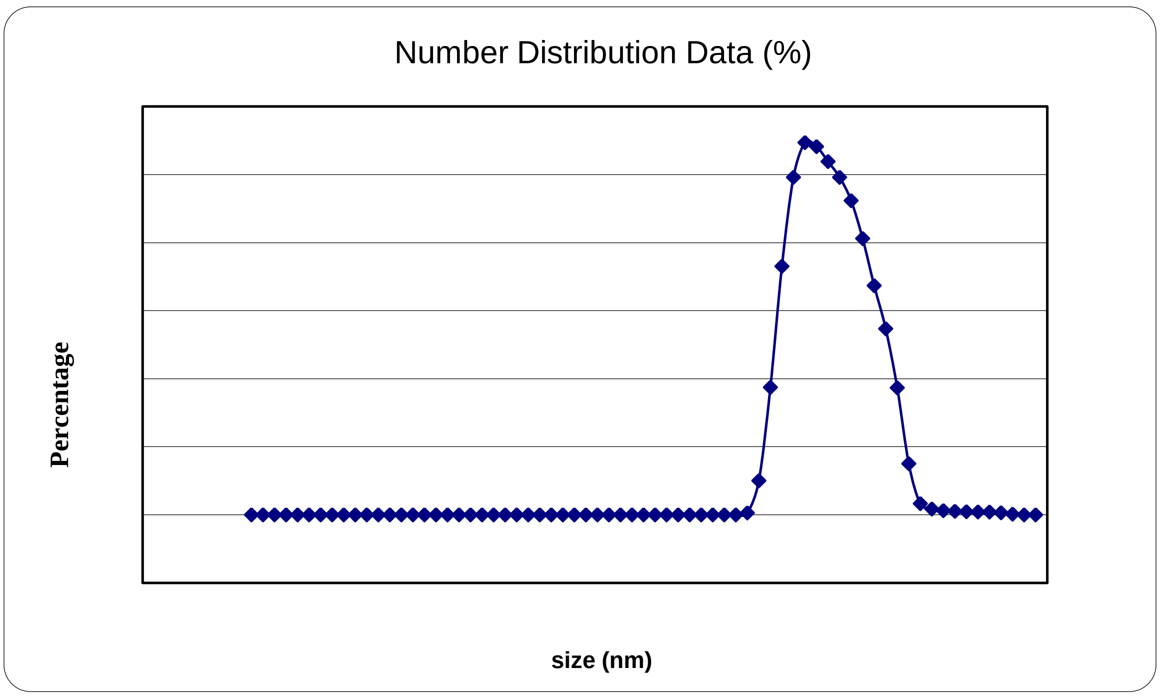

Figure-9: DLS Spectra of 0.1M Fe-doped TiO_2 Nanoparticles, (n-Hexane)

Photoluminescence analysis: Figure-10 showed the photoluminescence spectra of pure TiO_2 nanoparticles. Both spectra's showed the two distinct emission peaks, one peak occur in UV region while another peak occur in broad invisible green region. TiO_2 gives the spectral bands at 355-450 nm which should be ascribed to self-trapped excitons and oxygen vacancies respectively.

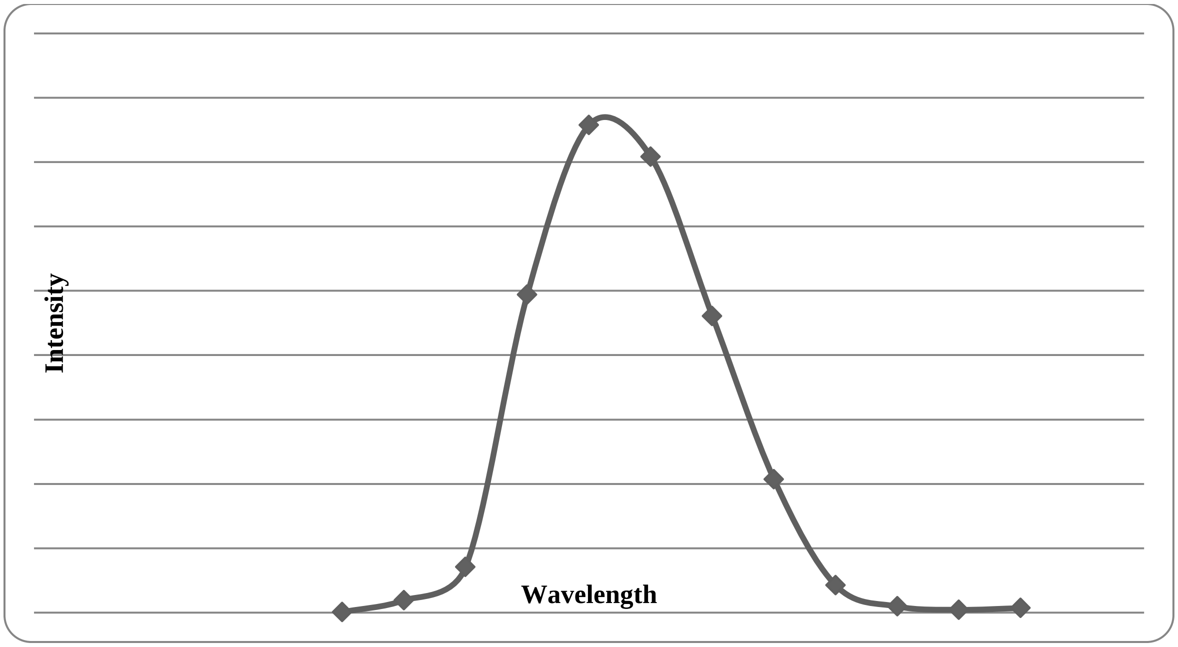

Figure-10: PL Spectra of TiO_2

Figure-11 showed the PL-spectra of 0.1M Fe-doped TiO_2 nanoparticles synthesized in 0.1M acetonitrile. The trapping of holes and electrons on surface of TiO_2donated to the Pl bands from 355-450 nm. From the spectra it can be seen that – OH group shows medium intensity with sharp peaks lies in the range of 355-370 nm. While broad luminescence band appeared in range of 370-450nm in blue green region. But PL-intensity was found different in all these samples which vary due to different solvents.

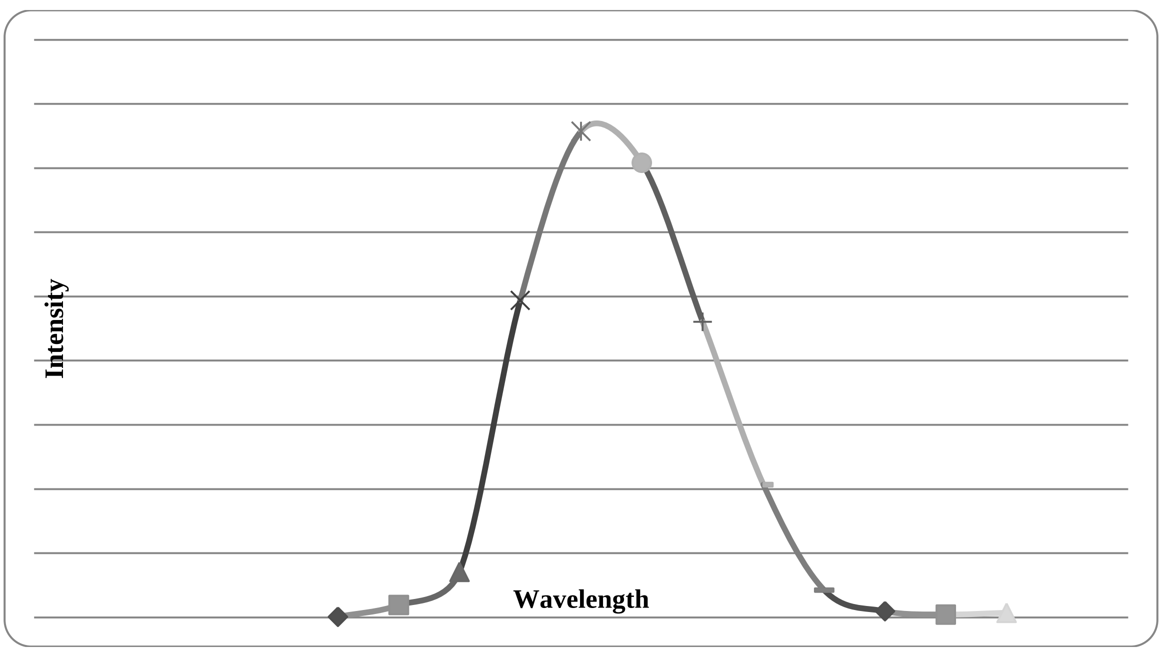

Figure-11:PL-Spectra of 0.1M Fe/TiO_2 Nanoparticles.

Antibacterial activity of Fe doped titanium oxides synthesized in various solvents: The antibacterial activity of Fe doped titanium oxides which were synthesized in various solvents such as acetonitrile, n-hexane and isopropyl alcohol was investigated against all strains *S. aureus* and *E. coli***.** Rifmpacin was used as standard in this study. The results from disc diffusion method showed that the nanoparticles synthesized in acetonitrile shown the highest inhibition 10 microgram/disc against *S. aureus* followed by nine microgram/disc inhibition nanoparticles synthesized in acetonitrile. While the lowest inhibition 8.5 microgram/disc was shown by the nanoparticles synthesized in isopropyl alcohol solvents. Whereas the used standard Rifmpacin 24 microgram/disc inhibition. The activity of these particles and was also performed against the inhibition of gram negative bacteria *E. coli* which showed the significant inhibition. The highest inhibition 10 microgram/disc was shown by the particles synthesized in isopropyl alcohol solvent followed 9 microgram/disc by n-hexane solvents. The particles synthesized in acetonitrile showed the lowest inhibition 8.5 microgram/disc against the gram negative bacteria while the standard sowed the highest 27 microgram/disc inhibition which is greater than the all particles. The results (fig-12) revealed that the overall significant inhibition against both tested bacteria's showed less than the standard used. The subscripts presented in graph shown rankwise comparison by HSD tucky comparison test. The other researchers also reported the significant antibacterial potential due to active oxygen spices, small size and high surface area (Sirelkhatim *et al*., 2015).

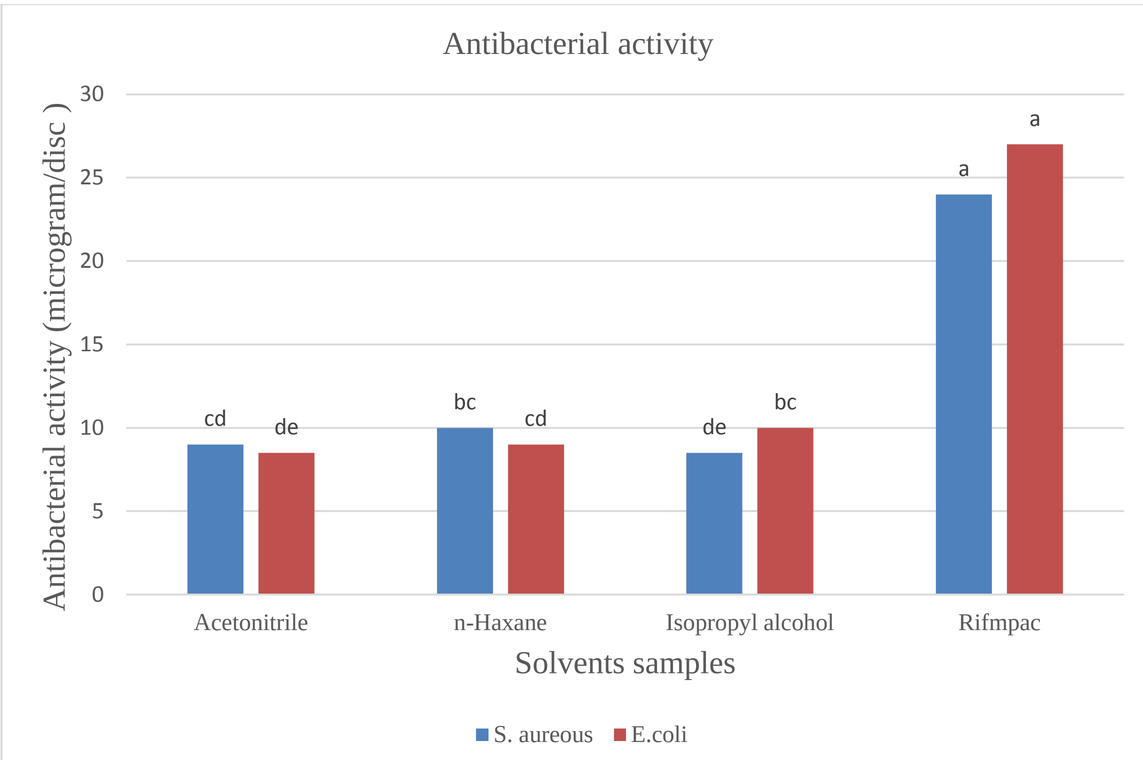

Figure-12: Antibacterial activity of Fe/TiO_2nanoparticles in various solvents

Antioxidant activity of Fe doped titanium oxides synthesized in various solvents: The antioxidant of Fe/TiO_2 was investigated by the DPPH scavenging assay by using ascorbic acid as standard.The obtained results were represented in Figure.13. The subscripts presented in graph shown rankwise comparison by HSD tucky comparison test. The nanoparticles synthesized in n-Hexane solvents showed the highest scavenging activity 25.34 % among all the synthesis solvents followed by isopropyl alcohol 21.61% while acetonitrile showed the lowest inhibition 20.17%. The lowest scavenging activity was shown by the acetonitrile. The ascorbic acid in n-hexane solvents showed the highest activity 73.54 %. The result showed that synthesis solvent influenced a little difference in scavenging activity but their overall activity was found less than the standard. Asati *et al*. (2009) also study the oxidase potential of cerium oxide nanoparticles which showed that the excellent antioxidant activity that leads to new potential applications in various fields such as medicine, environmental chemistry and biotechnology etc.

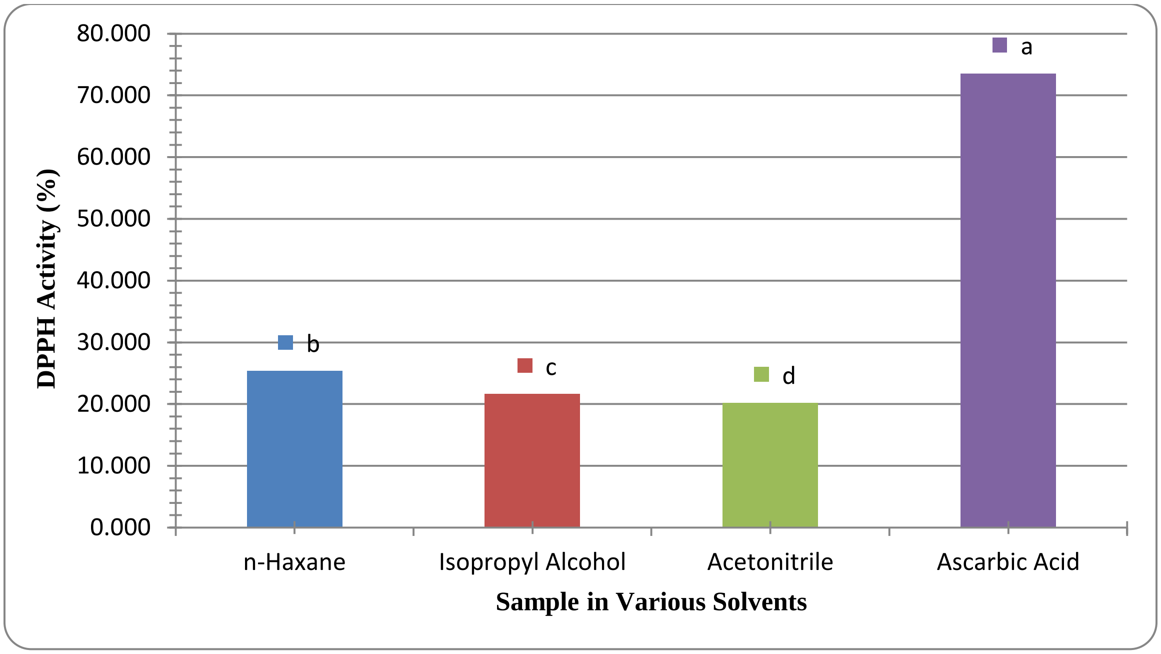

Figure-13: Percentage inhibition of DPPH radical activity of Fe/TiO_2nanoparticles in various solvents

Conclusion: The synthesized nanoparticles of size 20-30nm via sol-gel assay in three solvents like acetonitrile, n-haxane and isopropyl alcohol showed significant antioxidant and antibacterial activities.

REFERENCE

Afzal, M., M. Shahid, A. Jamil and S.U. Rehman. (2014). Phytochemical spectrum of essential oil of *Paganumharmala* by GC-MS and antimicrobial activity using sequential solvents fractions and essential oil. A. J. Chem. 26: 574-578.

Ahmadi, S.R. and N. Taghavinia. (2006). TiO_2 Nanostructured Films on Mica and Glass using chemical vapor deposition, First I. Congr. Nanosci. Nanotech., Tehran (Iran), 18-20.

Arshad, M., M.A. Farrukh, R.A. Sarfraz, A. Qayyum and S. Ali. (2016). Structural characterization of Fe/TiO_2 nanoparticles: antioxidant and antibacterial studies. Biointerf. Res. Appl. Chem. 6(5): 1497 – 1501.

Arshad, M., A. Qayyum, G. Abbas, R. Haider, M. Iqbal and A. Nazir (2018). Influence of different solvents on portrayal and photocatalytic activity of Tin-doped Zinc Oxide. J. Mol. Liq. 260: 272-278.

Asahi, R., T. Morikawa, T. Ohwaki, K. Aoki and Y. Taga (2001).Visible-light photocatalysis in nitrogen-doped titanium oxide. Sci. 293: 269-271.

Asati, A., S. Santra, C. Kaittanis, S. Nath and J.M. Perez (2009). Oxidase-like activity of polymer-coated cerium oxide nanoparticles. Angew. Chemie. 121(13): 2344-2348.

Attar, A.S., M.S. Ghamsari, F. Hajiesmaeilbaigi and S. Mirdamadi (2006). Template-based growth of TiO_2nanorods by sol-gel process, First I. Congr. Nanosci. Nanotech., Tehran (Iran). 18-20.

Babaei, N. (2006). Preparation of TiO_2/Al nanocomposite powders via the ball milling. First I. Congr. Nanosci. Nanotech., Tehran (Iran). 18-20.

Carnio, J.O., V. Teixeira, A. Portinha, A. Magalhaes, P. Coutinho, C.J. Tavares and R. Newton (2007). Iron doped photocaatalytic TiO_2 sputtered oatings applications. Mat. Sc. Eng. B. 138: 144-150.

Chen, X. and S.S. Mao (2007). Titanium dioxide nanomaterials: synthesis, properties, modifications and applications. Chem. Rev. 107: 2891-2959.

Chikhi, I., H. Allali and M.E.A. Dib (2012). Free radical scavenging and antibacterial activity of essential oil and solvent extracts of *Iris planifolia* (Mill) from Algeria. J. Med. Pl. Res. 6: 1961-1968.

Dessombz, A., D. Chiche, P. Davidson, P. Panine, C. Chaneac and J.P. Jolivet. (2007). Design of liquid-crystalline aqueous suspensions of rutile nanorods: Evidence of anisotropic photocatalytic properties. J. Amer. Chem. Soci. 129: 5904-5909.

Dozzi, M.V., S. Livraghi, E. Giamello and E. Selli (2011). Pho-tocatalytic activity of S- and F-doped TiO_2 in formic acid mineralization, Photochem. Photobio. Sci. 10: 343-349.

Du, Y.K., Y.Q. Gan, P. Yang, F. Zhao, N.P. Hua and L. Jiang (2005). Improvement in the heat-induced hydrophilicity of TiO_2 thin films by doping Mo(VI) ions. Th. Sol. Fil. 491: 133-136.

Fu, H., G. Shang, S. Yang and T. Xu (2012). Mechanistic study of visible-light-induced photodegradation of 4-chlorophenol by $TiO_2 - xNx$ (< x < 0.049) with low nitrogen concentration, I. J. Photoener. 1-9.

Fujishima A. and K. Honda. (1972). Electrochemical photolysis of water at a semiconductor electrode. Nat. 238: 37-38.

Fujishima, A., X. Zhang and D.A. Tryk (2008). TiO_2 photocatalysis and related surface phenomena. Surf. Sci. Reports, 63: 515-582.

Haghighat, F., A. Khodadadi and Y. Mortazavi (2006). Platinum and Ceria doped TiO_2 Nanoparticles prepared by microemulsion method and used for Oxygen sensor. First I. Congr. Nanosci. Nanotech., Tehran (Iran). 18-20.

Hajipour, M.J., K.M. Fromm, A.A. Ashkarran, D.J. Aberasturi, I.R. Larramendi, T. Rojo, V. Serpooshan, W.J. Parak and M. Mahmoud (2012). Antibacterial properties of Nanoparticles. Trend in biotech. 4:1-13.

Hoffmann, K.R., S.T. Martin, W. Choi and D.W. Bahnemann (1995). Environmental applications of semiconductor photocatalysis. Chem. Revi. 95: 69-96.

Hou, X., M. Huang, X. Wu and A. Liu (2009). First-principles calculations on implanted TiO_2 by 3d transition metal ions. Sci. China Series. 52: 838-842. (2009).

Jain, R. and S.K. Jain (2011). Total phenolic contents and antioxidant activities of some selected anticancer medicinal plants from Chhattisgarh State, India. Pharmacolog. 2: 755-762.

Jia, L., C. Wu, S. Han N. Yao, Y Li, Z. Li and L. Jian (2011). Theoretical study on the electronic and optical properties of (N, Fe)-codopedanatase TiO_2 photocatalyst. J. All. Comp. 509: 6067-6071.

Jung, H.S., J.K. Le, M. Nastasi, S.W. Lee, J.Y. Kim , J.S. Park and K.S. Hong (2005). Preparation 1F NanoporousMgO-coated TiO_2 nanoparticles and their application to the electrode of dye-sensitized solar cells. Langm. 21:10332-10335.

Lachheb H., E. Puzenat, A. Horas, M. Ksibi, E. Elaloui, C. Guillard and J.M. Herrmann (2002). Photocatalytic degradation of various types of dyes (Alizarin S, Crocein Orange G, Methyl Red, Congo Red, Methylene Blue) in water by UV-irradiated titania. App. Cata. B. 39: 75-90.

Li, X., X. Quan and C. Kutal (2004). Synthesis and photocatalytic properties of quantum confined titanium dioxide nanoparticle. Scr. Mat. 50: 499-505.

Lv, Y., L. Yu, H. Huang, H. Liu and Y. Feng (2009). Preparation, characterization of P-doped TiO_2nanoparticles and their excellent photocatalystic properties under the solar light irradiation. J. All. Comp. 488: 314-319.

Mangham, A.N., N. Govind , M.E. Bowden. V. Shutthanandan , A.G. Joly, M.A. Henderson and S.A. Chambers (2011). Photochemical properties, composition, and structure in molecular beam epitaxy grown Fe “Doped” and (Fe,N) Co doped Rutile TiO_2. J. Phys. Chem. *C*. 115: 15416–15424.

Naceur, J.B., R. Mechiakh, F. Bousbih and R. Chtourou (2011). Influences of the iron ion (Fe^{3+})–doping on structural and optical properties of nanocrystalline TiO_2 thin films prepared by sol-gel spin coating, App. Sur. Sci. 257: 10699-10703.

Naeem, K. and F. Ouyang (2011). Preparation of Fe^{3+} -doped TiO_2 nanoparticles and its photocatalytic activity under UV light. Phy. B. 405: 221-226.

Qayyum, A., R.A. Sarfraz, A. Ashraf and S. Adil (2016). Phenolic composition and biological (anti diabetic and antioxidant) activities of different solvent extracts of an endemic plant (*Heliotropium strigosum*). J. Chil. Chem. Soci. 61(1): 2828-2831.

Rehman, A., S. Ullah, R.A. Sarfraz, F. Nawaz, A. Qayyum, M. Javid, S.M.I. Riaz and K. Khan (2017). Evaluation of thrombolytic, antimicrobial and cytotoxicity potential of extract and its polar fractions of Heliotropium strigosum by in-vitro assay. I. J. Biosci. 10(1):109-116.

Rella, R., J. Spadavecchia, M.G. Manera M.G., Capone, S., A. Taurino, M. Martino, A.P. Caricato and T. Tunno (2007). Acetone and ethanol soled-stage gas sensors based on TiO_2 nanoparticles thin film deposited by matrix assisted pulsed laser evaporation. Sens. Actuat. B. 127: 426-431.

Sarkar, D., C.K. Ghosh, U.N. Maiti and K.K. Chattopadhyay (2011). Effect of spin polarization on the optical properties of Co-doped TiO_2 thin films. Phy. B. 406: 1429-1435.

Sirelkhatim, A., S. Mahmud, A. Seeni, N.H.M. Kaus, L.C. Ann, S.K.M. Bakhori and D. Mohamad (2015). Review on zinc oxide nanoparticles: antibacterial activity and toxicity mechanism. Nano-Micro Lett. 7(3): 219-242.

Sontakke, S., C. Mohan, J. Modak and G. Madras (2012). Visible light Photocatalytic inactivation of Escherichia coli with combustion synthesized TiO_2. Chem, Eng. J. 101-107.

Stan, M., A. Popa, D. Toloman, A. Dehelean, I. Lung and G. Katona (2015). Enhanced photocatalytic degradation properties of zinc oxide nanoparticles synthesized by using plant extracts. Mat Sc Semicond. Proces. 39:23-29.

Su,Y., Y. Xiao, Y. Li, Y. Du and Y. Zhang (2011). Materials Preparation, photocatalytic performance and electronic structures of visible-light-driven Fe–N-Co doped TiO2 nanoparticles. Mat. Chem.Phys. 126(3):761-768.

Subramanian, M., S. Vijayalakshmi, S. Venkataraj and R. Jayavel (2008). Effect of cobalt doping on the structural and optical properties of TiO_2 films prepared by sol-gel process. Thin Sol. Fil. 516: 3776-3782.

Testino, A., I.R. Bellobono and V. Buscaglia (2007). Optimizing the photocatalytic properties of hydrothermal TiO_2 by the control of phase composition and particle morphology. A systematic approach. J. Amer. Chem. Soci., 129: 3564-3575,

Thompson T.L. and J.T. Yates (2006). Surface science studies of the photoactivation of TiO_2 –new photochemical processes. Chem. Rev. 106: 4428-4453.

Tojo, S., T. Tachikawa, M. Fujitsuka and T.O. Majima (2008). Iodine-Doped TiO_2 Photocatalysts: Correlation between Band Structure and Mechanism. *J. Phys. Chem. C.* 112: 14948–14954.

Tsuyumoto, I. and K. Nawa (2008). Thermochromism of vanadium titanium oxide prepared from peroxovanadate and peroxotitanate. J. Mater. Sci., 43:985-988.

Umebayashi, T., T. Yamaki, H. Itoh and K. Asai (2002). Band gap narrowing of titanium dioxide by sulfur doping. App. Phy. Lett. 81: 454-456.

Wang, C., C. Shao, Y. Liu and X. Li (2009). Water-dichloromethane interface controlled synthesis of hierarchical rutile TiO_2 superstructures and their photocatalytic properties. Inorg. Chem. 48: 1105-1113.

Wang, J., Z. Liu and R. Cai (2008). A new role for Fe+3 in Tio_2hydrosol acceleratedphotodegration of dyes under visible light. Envir. Sci. Tech. 42: 5759-5764.

Wang, M. C., H.J. Lin and T.S. Yang (2009). Characteristics and optical properties of iron ion (Fe^{3+})-doped titanium oxide thin films prepared by a sol-gel spin coating. J. All. Comp. 473: 394-400.

Wang, Y., L. Zhang, K. Deng, X. Chen and Z. Zou (2007). Low temperature synthesis and photocatalytic activity of rutile TiO_2nanorod superstructures. J. Phys. Chem. C. 111: 2709-2714.

Weng, W., M. Ma and P. Du (2005). Superhydrophilic Fe doped titanium dioxide thin films prepared by a spray Pyrolysis deposition. Surf. Coat. Tech. 198: 340-344.

Yalc, Y., M. Kilic and Z.C. Inar (2010). Fe+ 3-doped TiO2: A combined experimental and computational approach to the evaluation of visible light activity. App. Cataly. B: Envir. 99(3-4): 469-477.

Yang, H. G., C.H. Sun, S.Z. Qiao, J. Zou, G. Liu, S. C. Smith, H. M. Cheng and G. Q. Lu (2008). Anatase TiO_2 single crystals with a large percentage of reactive facets. Nat. 453: 638-641.

Yu, H., K. Zhang and C. Rossi (2007). Experimental Study of the Photocatalytic Degradation of Formaldehyde in Indoor Air using a Nano-particulate Titanium Dioxide Photocatalyst. Indoor Built Envir. 16: 529-537.

Yu, J.C., L. Zhang and J. Yu (2002). Direct sonochemical preparation and characterization of highly active mesoporous TiO_2 with a bicrystalline framework. Chem. Mater. 14: 4647-4653.

Zhang, H., H. Liu, C. Mu and D. Qiu, D (2006). Antibacterial properties 1f nanometer Fe^{3+}-TiO_2 thin films. IEEE I. Conf. Nano. Mecro. Eng. and Mol. Sys. 955-958.

Zhang, J., Q. Xu, Z. Feng, M. Li. and C. Li (2008). Importance of the relationship between surface phases and photocatalytic activity of TiO_2. Angew. Chem. I. Edit. 47:1766-1769.

Zhang, J., Y. Wu, M. Xing, S.A. K. Leghari and S. Sajjad (2001). Development of modified N doped TiO_2photocatalyst with metals, nonmetals and oxides. Ener. Envir. Sci. 3: 715-726.

Zhang, Y., Y. Shen, F. Gu, M. Wu, Y. Xie and J. Zhang (2009). Influence of Fe ions in characteristics and optical properties of mesoporous titanium oxide thin films. Appl. Surf. Sci. 456: 85-89.

Zhou, M. J. Yu and B. Cheng (2006). Effects of Fe-doping on the photocatalytic activity of mesoporous TiO_2 powders prepared by an ultrasonic method. J. Hazard. Mat. 137: 1838-1847.

Zhou, M., J. Zhang, B. Cheng and H. Yu. (2012). Enhancement of visible-light photocatalytic activity of mesoporous Au-TiO_2 nanocomposites by surface plasmon resonance. I. J. Photoener. 1-10.

Zhu, H., X. Gao, Y. Lan, D. Song, Y. Xi and J. Zhao (2004). Hydrogen titanatenanofibers covered with anatasenanocrystals: a delicate structure achieved by the wet chemistry reaction of the titanatenanofibers. J. Amer. Chem. Soci., 126: 8380-8381.